

Energy Levels of N^{14} from $N^{15}(\text{He}^3, \alpha)N^{14*}\dagger$

DONALD D. CLAYTON

California Institute of Technology, Pasadena, California

(Received July 16, 1962)

The energy level scheme of N^{14} in the 4–8 MeV range of excitation has been examined by measuring the alpha-particle spectrum from the reaction $N^{15}(\text{He}^3, \alpha)N^{14*}$. States are observed at N^{14} excitations of 3.95, 4.91, 5.113 ± 0.008 , 5.691 ± 0.008 , 5.832 ± 0.008 , 6.048 ± 0.012 , 6.224 ± 0.012 , 6.436 ± 0.012 , 7.032 ± 0.010 , 7.97, and 8.06 MeV. Unobserved are the now doubtful states reported near 6.70, 7.40, and 7.60 MeV in N^{14} . The implications of a possible state near 7.60 on the C^{12}/C^{13} abundance ratio are discussed and it is concluded that observed isotope abundance ratios are consistent with the finding of this experiment; that is, that such a level does not exist. Angular distributions are presented which show the evidence of different reaction mechanisms to different final states. The reaction $N^{14}(\text{He}^3, \alpha)N^{13*}$ also produced resolvable alpha-particle groups to states in N^{13} with excitations of 6.38, 6.91, 7.16 ± 0.008 , and 7.388 ± 0.008 MeV.

I. INTRODUCTION

THERE exists at present considerable uncertainty in both the number of excited N^{14} states in the 6–8 MeV excitation range and in their excitation energies. This lack of information results from the relative inaccessibility of this energy region to low-energy charged-particle reactions. The Q values for the commonly investigated charged-particle reactions leading to N^{14} final states are for the most part too low, whereas the excitation of N^{14} in those reactions for which it is the compound nucleus all lie too high. The reaction to be reported in the present study, $N^{15}(\text{He}^3, \alpha)N^{14}$, can easily populate that excitation range of N^{14} , having an energy release of 9.743 MeV.

The reported information for N^{14} states in the energy region 6–8 derives mainly from inelastic scattering experiments and neutron and gamma-ray spectroscopy. The inelastic scattering of 22-MeV alpha particles was studied by Miller *et al.*¹ They found excitation energies in N^{14} of 6.47, 7.02, and 7.94 MeV which must of necessity have large $T=0$ components. Burge and Prowse² have observed the inelastic scattering of protons with photographic emulsions and report levels below 7.7 MeV at 6.23, 6.46, 6.60 (doubtful), 7.02, 7.40, and 7.60 MeV. The last level is of particular interest because it could provide a possible resonance in the $C^{13}(p, \gamma)N^{14}$ reaction in stellar interiors. The kinematics of the inelastic proton experiment, however, were such as to prevent identification of the last two levels at a convincing variety of angles. An additional puzzle arises from the inexplicably large yield of inelastic protons to the assumed 7.60-MeV level when compared to the yield to the 7.02-MeV level. The close similarity of the interaction Hamiltonians for inelastic proton scattering and inelastic alpha scattering would lead one to expect

the appearance of the 7.60-MeV level in inelastic alpha scattering (unless $T=1$) in contradiction to the observations. Benenson³ has observed neutrons from $C^{13}(d, n)N^{14}$ and reports levels at 6.23, 6.43, 7.00, 8.08 MeV, as well as a level at 7.72 MeV and a possible one at 7.50-MeV excitation in N^{14} . There is a temptation to identify the possible states at 7.50 and 7.72 MeV with the ones reported at 7.40 and 7.60 MeV from the inelastic proton scattering experiment. Such an identification would seem rather arbitrary in the face of the relatively small error quoted by both investigators and the close agreement on Q values to the other observed states. This doubt is not resolved by the gamma-ray spectrum of N^{14} , as observed by Bent *et al.*⁴ with $C^{13}(d, n)N^{14}$. They found an unassignable gamma ray of 7.30 MeV.

Hebbard and Vogl⁵ have measured the cross section for $C^{13}(p, \gamma)N^{14}$ down to proton energies of 100 keV and have established the existence of N^{14} states at 7.97- and 8.06-MeV excitation. Their yields decrease smoothly with decreasing bombarding energies, showing no evidence of other lower lying states. By calculating proton widths for various possible l -wave resonances and observing that levels with spins up to $J=3$ exist below 7-MeV excitation for possible gamma-ray cascades, they conclude that any resonance for which $J \leq 5$ would probably have been observed. This argument makes the existence of any state in the 7.64–7.96 excitation range unlikely. It should be noted that this range of excitation includes the 7.72-MeV level reported by Benenson.

In summary, it may be stated that the existing evidence on states in N^{14} in the excitation range 6.2–8.4 MeV indicates conclusively the existence of states at 6.23, 6.44, 7.03, 7.97, and 8.06 MeV. The evidence for states at 6.6, 7.3, 7.4, 7.6, and 7.7 MeV appears to be subject to valid doubt.

II. $C^{13}(p, \gamma)N^{14}$ IN STELLAR INTERIORS

It has already been mentioned that a reported state near 7.60 MeV excitation in N^{14} could serve as a possi-

[†] Supported in part by the joint program of the Office of Naval Research and the U. S. Atomic Energy Commission. This paper presents results of one phase of research carried out at the California Institute of Technology under Contract NASW-6 (WO 98001) sponsored by the National Aeronautics and Space Administration.

¹ D. W. Miller, B. M. Carmichael, U. C. Gupta, V. K. Rasmussen, and M. B. Sampson, *Phys. Rev.* **101**, 740 (1956).

² E. J. Burge and D. J. Prowse, *Phil. Mag.* **1**, 912 (1956).

³ R. E. Benenson, *Phys. Rev.* **90**, 420 (1953).

⁴ R. D. Bent, T. W. Bonner, and R. F. Sippel, *Phys. Rev.* **98**, 1237 (1955).

⁵ D. F. Hebbard and J. L. Vogl, *Nuclear Phys.* **21**, 652 (1960); and J. L. Vogl (private communication).

ble resonance for the $C^{13}(p, \gamma)N^{14}$ reaction in stellar interiors. $C^{13}+p$ lies at 7.549 MeV in N^{14} and any state lying in the first 100 keV above that value must be considered as having a potential effect on the $C^{13}(p, \gamma)N^{14}$ reaction rate. This reaction rate is instrumental in determining the amount of C^{13} that can persist in stellar interiors.

There exist many stars in which the C^{12}/C^{13} abundance ratio is measurable using the techniques of molecular band spectra.⁶ This ratio is a valuable aid in determining the history of the star in light of the mechanisms of element synthesis. The production of C^{13} results from the reaction $C^{12}(p, \gamma)N^{13}(\beta^-)C^{13}$ when carbon is present in stellar interiors at temperatures of about 10^7 °K and higher. Under slowly changing conditions, the sequence of reactions called the CNO cycle will occur. Burbidge *et al.*⁷ have studied this cycle in detail. When hydrogen burning occurs for a time that is long compared to the time for one cycle, the net effect is the production of He^4 from protons with the added result that the CNO nuclei will be processed to an equilibrium abundance ratio. The equilibrium abundance of each CNO nucleus is inversely proportional to the reaction rate per nucleus of the reaction which destroys that nucleus. Under the assumption that the two reactions, $C^{12}(p, \gamma)N^{13}$ and $C^{13}(p, \gamma)N^{14}$, are both nonresonant at stellar energies, the equilibrium abundance ratio is calculated to be⁵ $C^{12}/C^{13}=4.1$. Whereas the $C^{12}(p, \gamma)N^{13}$ reaction is certainly nonresonant at stellar energies, the situation regarding the $C^{13}(p, \gamma)N^{14}$ reaction is clouded by the uncertainties of the N^{14} energy level scheme. Not only would the nonresonant extrapolation of the reaction rate be in error if an appropriate resonance exists, but a rather complicated temperature dependence would also enter into the C^{12}/C^{13} abundance ratio. This problem exists even for high l -wave resonances.

The magnitude of the effect of possible resonances can be estimated using the development and notation of the review of Burbidge *et al.*⁷ Charged-particle reactions in stars essentially take place in a range of interaction energies ΔE_0 centered about the effective stellar energy, E_0 , at which the product of the Maxwell-Boltzmann velocity distribution and the Gamow penetration factor has a maximum value. For the $C^{13}(p, \gamma)N^{14}$ reaction, $E_0 = 3.94 T_6^{2/3}$ and $\Delta E_0 = 1.35 T_6^{5/6}$, where the energies are in keV and the temperature T_6 is in millions of degrees. Under the assumptions that a resonance exists in $C^{13}(p, \gamma)N^{14}$ in the proton energy range $E_0 - 2\Delta E_0 < E_r < E_0 + 2\Delta E_0$ and that $\Gamma_\gamma > \Gamma_p$ for such low bombarding energies, the number of reactions per cm^3 per second is

TABLE I. Characteristic values for the ratio P_r/P_{nr} for various l -wave resonances in $C^{13}(p, \gamma)N^{14}$ at two different stellar temperatures.

$T_6=20$	$l=0$	$l=1$	$l=2$
$E_r=54$	4.2×10^3	490	7.8
$E_r=64$	77	9.0	0.1
$T_6=36$	$l=0$	$l=1$	$l=2$
$E_r=54$	3.5×10^5	3.8×10^4	650
$E_r=100$	84	9.1	0.1

$$P_r = 1.09 \times 10^{40} \rho^2 \frac{\chi_H \chi_{13}}{A_H A_{13}} \frac{\omega f_r \theta_p^2}{K_{2l+1}^2(3.0)} T_6^{-3/2} \times \exp[-(181.5 E_r^{-1/2} + 11.61 E_r / T_6)], \quad (1)$$

where the resonance energy E_r is in keV, χ is the fraction by weight of a given nuclear species in the star, and f_r is an enhancement factor at resonance due to the shielding by electrons of the Coulomb repulsion. If no such resonance exists, the low-energy proton capture occurs primarily into the tail of the broad s -wave resonant state at 8.06 MeV in N^{14} with an extrapolated cross-section factor $S_0 = 6.0$ keV-b.⁵ The corresponding nonresonant reaction rate in stellar interiors is

$$P_{nr} = 5.32 \times 10^{33} \rho^2 \frac{\chi_H \chi_{13}}{A_H A_{13}} f_0 T_6^{-2/3} \exp[-(137.2 T_6^{-1/3})]. \quad (2)$$

The extent of the error in the nonresonant abundance ratio due to a resonance can be estimated by the ratio of these two reaction rates. Assuming that the electron-shielding factors, f_0 and f_r , are equal, this ratio reduces to

$$\frac{P_r}{P_{nr}} = 2.06 \times 10^6 \frac{\omega \theta_p^2}{K_{2l+1}^2(3.0)} T_6^{-5/6} \times \exp[-(181.5 E_r^{-1/2} + 11.61 E_r / T_6 - 137.2 T_6^{-1/3})]. \quad (3)$$

Table I lists a few values for the ratio P_r/P_{nr} for three different l -wave resonances and for the two temperatures $T_6=36$ and $T_6=20$. The statistical factor ω has been set equal to unity and the dimensionless reduced proton width θ_p^2 has been assumed to be 1%. The value $E_r=54$ keV has been listed for both temperatures since it corresponds to the reported N^{14} state near 7.60-MeV excitation. This short table reveals the strong dependence of the $C^{13}(p, \gamma)N^{14}$ reaction rate on both the temperature and the resonance energy. Since $C^{12}/C^{13} \simeq 4.1(1 + P_r/P_{nr})$, it is evident that the relative amount of C^{13} could be greatly decreased by a resonance in the first 100 keV above $C^{13}+p$.

Regarding the evidence obtained from the carbon stars, McKellar⁶ says:

"Summarized, the present state of knowledge on the carbon isotopes in the atmospheres of the cool carbon stars is as follows: (1) There is a group of R -type stars

* A. McKellar, in *Stellar Atmospheres*, edited by J. L. Greenstein (University of Chicago Press, Chicago, Illinois, 1960); see Chap. 16. References to experimental determinations of C^{12}/C^{13} are given there.

⁷ E. M. Burbidge, G. R. Burbidge, W. A. Fowler, and F. Hoyle, *Revs. Modern Phys.* **29**, 547 (1957). See also W. A. Fowler, *Mém. Soc. Roy. Sciences de Liège* **14**, 88 (1954); and **16**, 207 (1960); G. R. Caughlan and W. A. Fowler, *Astrophys. J.* (to be published).

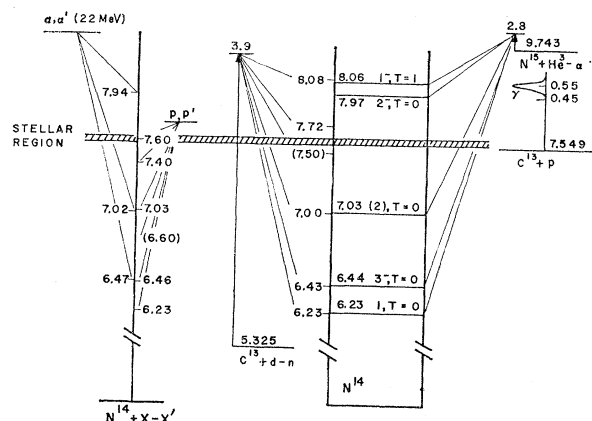


FIG. 1. Evidence for states in N^{14} in the 6–8 MeV range of excitation. The pertinent reactions are $N^{14}(\alpha, \alpha')N^{14*}$, $N^{14}(p, p')N^{14*}$, $C^{13}(d, n)N^{14*}$, $C^{13}(p, \gamma)N^{14}$, and the present experiment, $N^{15}(\text{He}^3, \alpha)N^{14*}$. The stellar energy region for effective resonances in $C^{13}(p, \gamma)N^{14}$ is indicated by a horizontal band.

for which the C^{12}/C^{13} abundance ratio is about 100 or more; (2) for the remainder of the R -type stars for which measurements can be made with some confidence, those on the 1, 0 band of C_2 appear to yield a fairly constant C^{12}/C^{13} ratio of about 5; (3) for the N -type stars, results by various investigators from a wider variety of bands give C^{12}/C^{13} ratios in the range from about 20 to 2."

It is important to realize that the C^{12}/C^{13} abundance ratio may be arbitrarily large due to a superposition of C^{12} from helium burning with the carbon that has been processed in the CNO cycle. It is the smallest observed C^{12}/C^{13} ratios that must be compared to the ratio expected from the CNO cycle. It is clear that the observations are reasonably consistent with the C^{12}/C^{13} ratio expected if no resonance exists in $C^{13}(p, \gamma)N^{14}$ at stellar energies. If an appropriate resonance does exist, a completely different mechanism for the production of C^{13} will be required to explain the large amounts of C^{13} observed in these carbon stars. Figure 1 presents a schematic summary of the existing evidence on N^{14} energy levels above 6.2 MeV. Also indicated is the energy region in which an N^{14} level would be likely to influence the $C^{13}(p, \gamma)N^{14}$ reaction rate in stellar interiors.

III. SUITABILITY OF THE $N^{15}(\text{He}^3, \alpha)N^{14*}$ REACTION

It is clearly desirable to examine the 6–8 MeV excitation range of N^{14} with a low-energy charged-particle reaction of high resolution. For bombarding energies of 3 MeV or less, the only suitable reaction available is $N^{15}(\text{He}^3, \alpha)N^{14}$ with a Q value of 9.743 MeV from mass differences.⁸ Outgoing alpha particles leaving N^{14} with an excitation of about 8 MeV will also have energies of the order of 3 MeV. These energies are suitable for high resolution measurements.

⁸ F. Everling, L. A. Konig, J. H. E. Mattauch, and A. H. Wapstra, *Nuclear Phys.* **18**, 529 (1960).

Three possible models or mechanisms for reactions such as $N^{15}(\text{He}^3, \alpha)N^{14}$ are in common usage: (a) compound nucleus formation, (b) neutron pickup, and (c) heavy-particle direct interactions. In terms of compound nucleus formation, $N^{15} + \text{He}^3$ lies at 14.16 MeV in F^{18} . The density of broad $T=0$ and $T=1$ levels at F^{18} excitations greater than that energy is probably high, and the reaction may proceed through several overlapping levels of unknown spins and parities. Such a situation would, in general, be favorable for emission of alpha particles to a wide variety of quantum states for the residual excited N^{14} nucleus. Excitation functions obtained for this reaction to a variety of final N^{14} states revealed no predominant resonant structure that might favor population of certain final N^{14} states at the expense of others. In the range of bombarding energies $2.2 < E < 2.8$ the cross section is a smooth and slowly rising function of increasing bombarding energy. The neutron pickup mechanism could be effective to those N^{14} states that can be described in terms of the direct removal of a neutron from the N^{15} ground-state configuration. That is, the configuration s^4p^{10} of N^{14} may be populated in this manner. In a theoretical analysis of N^{14} , Warburton and Pinkston⁹ conclude that the only likely members of this configuration below 9 MeV are the N^{14} ground state, the 2.13-MeV level, the 3.95-MeV level, and a level with $(J^\pi, T) = (2^+, 0)$, which they tentatively identify as the 7.03-MeV level on the basis of gamma-ray evidence. The possibility of heavy-particle stripping is even harder to evaluate. It will, in general, be proportional to the probabilities that the N^{15} ground state and the final N^{14} excited state can be described, respectively, in terms of a bound (B^{11}, He^4) cluster and a bound (B^{11}, He^8) cluster. Owen and Madansky¹⁰ find, for example, that the alpha-particle angular distribution from $C^{13}(\text{He}^3, \alpha)C^{12}$ can be accounted for by a rather complicated interference between neutron pickup and heavy-particle stripping amplitudes. It would seem, at any rate, that the available variety of reaction mechanisms would improve the chance of populating all the excited states of N^{14} below 8 MeV.

A generally favorable situation is also presented by charged-particle penetrabilities. Although the Coulomb barrier for $N + \text{He}$ is relatively large (3.2 MeV), the penetrability is reasonably insensitive to the angular momentum barrier. From the tables of Schiffer¹¹ for an alpha-particle energy of 2.4 MeV, the penetrability ratios are found to be $P_0:P_1:P_2:P_3 = 1.0:0.74:0.35:0.10$. These ratios insure that population of final states will not be greatly hindered by the angular momentum barrier.

⁹ E. K. Warburton and W. T. Pinkston, *Phys. Rev.* **118**, 733 (1960).

¹⁰ G. E. Owen and L. Madansky, Atomic Energy Commission Report NYO-2054, 1958 (unpublished).

¹¹ J. P. Schiffer, Argonne National Laboratory Report ANL-5739, 1957 (unpublished).

IV. EXPERIMENTAL ARRANGEMENT

The experiment was conducted on the Kellogg Radiation Laboratory 3-MV electrostatic accelerator. The He^3 -beam energy was determined by a 90° electrostatic analyzer. A beam energy of 2.763 ± 0.003 MeV was used throughout this experiment except for the excitation functions measured as a function of bombarding energy. The reaction products were momentum analyzed by a 16-in.-radius double-focusing magnetic spectrometer. A momentum resolution $p/\delta p = 231$ and a spectrometer solid angle of 6.3×10^{-3} sr were used throughout. It was necessary to determine the type of particle by a pulse-height analysis at the exit focus of the magnetic spectrometer. For this purpose, a p - n junction particle detector was used in conjunction with thin foils. For relatively low-energy particles passing through the spectrometer ($E_\alpha = E_p \sim 3$ MeV), a thin foil was placed in front of the detector to lower the alpha-particle pulse height to a size intermediate to the proton and deuteron pulse size. For the higher energy part of the momentum spectrum ($E_\alpha = E_p \sim 5$ MeV), the detector bias was lowered to a point such that the depletion layer of the counter was insufficient to stop the protons. In both methods a clear separation of the various particle types was obtained, the spectra having been stored in a 100-channel pulse-height analyzer. It should be emphasized that the energy of the reaction products was determined by their spectrometer momenta, and that pulse-height analysis was used only for identification of particle types.

The nitrogen targets used in this experiment consisted of a thin layer of TiN on a nickel backing. Titanium was first evaporated onto a nickel backing, and the resultant thin layer was nitrided by induction heating to a red heat for a short time in an atmosphere of dry ammonia. The resulting TiN compound is stable under bombardment. The ammonia for the N^{15} target was prepared from ammonium nitrate, supplied by the Eastman Kodak Company, with the ammonium radical enriched in N^{15} to 67%. A similar N^{14} target was prepared by the same procedure using natural ammonia, and was used to determine that part of the reaction spectrum which originates from N^{14} in the first target. The thickness of the TiN layer was measured by observing the resonance profile of the $N^{15}(p, \alpha\gamma)C^{12}$ yield as a function of bombarding energy. The integrated alpha yield from the same reaction also measured the total number of N^{15} atoms per square centimeter in the target. The TiN layer contained 1.9×10^{17} N^{15}/cm^2 and was 7 keV thick for 429-keV protons, corresponding to 18 keV for the He^3 beam used in this experiment. The natural nitrogen target contained 1.6×10^{17} N^{14}/cm^2 .

The magnetic spectrometer was calibrated against the incident He^3 energy during each run by a variety of techniques which gave reproducible and consistent results within the resolution of the spectrometer. From the carbon which built up on the surface of the target came protons of known energy from $C^{12}(\text{He}^3, p)N^{14}$ to

the first three states of N^{14} and alpha particles of known energy from $C^{12}(\text{He}^3, \alpha)C^{11}$. The reaction $C^{12}(\text{He}^3, p)N^{14}$ was also used to monitor the amount of carbon buildup on the target surface using the cross sections of Bromley *et al.*¹² By inserting small amounts of hydrogen into the He^3 ion source, it was possible to obtain small components of H_3^+ and HD^+ ions with the He^3 beam. This insertion caused the alpha particles from $N^{15}(p, \alpha)C^{12}$ to appear in the reaction spectrum as a further convenient calibration energy. The largest uncertainties in the measured Q values arise from the energy-loss connections in the surface carbon layer and from the poor momentum profiles of some final states due to overlap or low yields.

Cross sections were calculated from the thin-target integrated yield formula¹³

$$\frac{d\sigma}{d\Omega} = \frac{1}{n_1 n_0} \frac{R}{\Omega} \int \frac{Y(p) dp}{p}, \quad (4)$$

where n_1 and n_0 are the number of projectiles and the number of target atoms per cm^2 , R is the momentum resolution of the spectrometer of solid angle Ω , and $Y(p)$ is the yield of alpha particles at momentum p . For the spectrometer used in this experiment, the momentum is measured by the voltage drop V_m across a standard resistor through which the current to a mechanical fluxmeter coil passes. V_m is inversely proportional to the corresponding particle momentum, and the kinetic energy of particles passing through the spectrometer is numerically $E(\text{MeV}) = 0.40/V_m^2$. The yields obtained will be plotted against V_m .

In two instances, the profile of an observed alpha group had sufficient energy breadth to allow calculation of the width of the final state being populated. In these cases it was assumed that the spectrometer resolution and the target thickness combined to produce a Gaussian viewing window of known width which was folded with a Gaussian width for the final state to produce the observed width of the alpha group profile.

V. ALPHA PARTICLE SPECTRUM

The bulk of the data to be reported consists of the yield of alpha particles as a function of their momenta as determined by the magnetic spectrometer. The range of alpha-particle energies observed was such as to include the group from $N^{15}(\text{He}^3, \alpha)N^{14}$ (3.95 MeV) at the high-energy end and the group from $N^{15}(\text{He}^3, \alpha)N^{14}$ (8.06 MeV) at the low-energy end. The spectra were measured for a bombarding He^3 energy of 2.763 MeV at laboratory angles of 150° and 90° , both with the 67% N^{15} target and with the natural nitrogen target. The latter target was used to determine the alpha spectrum from $N^{14}(\text{He}^3, \alpha)N^{13}$, a necessary identification procedure since

¹² D. A. Bromley, E. Almqvist, H. E. Gove, H. E. Litherland, E. B. Paul, and A. J. Ferguson, *Phys. Rev.* **105**, 957 (1957).

¹³ A. B. Brown, C. W. Snyder, W. A. Fowler, and C. C. Lauritsen, *Phys. Rev.* **82**, 159 (1951).

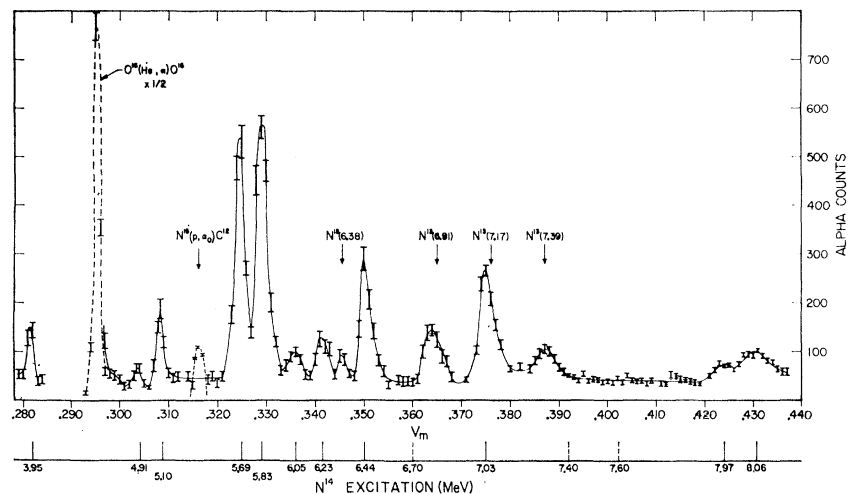


FIG. 2. The spectrum of alpha particles at $\theta_L = 150^\circ$ from bombardment of a 67% N^{15} target of TiN with 2.76-MeV He^3 ions. The error bars represent $\pm\sqrt{n}$ counting statistics, the yields having been normalized to 500 μC of He^{3+} ions. Alpha-particle energies corresponding to specific excitations of the residual N^{14} nucleus are indicated on the lower abscissa. Reaction groups due to contaminants are noted by arrows above the yield curve. $E_\alpha = 0.40/V_m^2$.

N^{14} accounts for 1/3 of the nitrogen in the N^{15} enriched target. Since the natural nitrogen target contains 1.7 times as many N^{14}/cm^2 as the N^{15} enriched target, peaks from $N^{14}(He^3, \alpha)N^{13}$ appear with both targets but with a correspondingly greater yield from the natural nitrogen target.

Figures 2 and 3 show the 150° spectra from the enriched N^{15} target and the N^{14} target, respectively, and Fig. 4 shows the spectrum at 90° from the enriched N^{15} target. The number of alpha-particle counts at each magnetic spectrometer setting V_m ($E_\alpha \approx 0.40/V_m^2$) has been normalized to 500 μC of He^{3+} bombardment. The error bars represent $n \pm (n)^{1/2}$ before normalization to that value of integrated bombardment. The expected momenta of the various $N^{15}(He^3, \alpha)N^{14}$ alpha groups are located on a second abscissa labeled with the excitation of the residual nucleus just below the abscissa V_m . The expected momenta of additional alpha groups from $N^{14}(He^3, \alpha)N^{13}$ and from carbon and oxygen contaminants are indicated by arrows above the yield curve, which is drawn by the well-known technique of author's bias.

Although the general nature of the spectrum can be seen from Figs. 2-4, several comments are in order before tabulating the results. The alpha-particle group

from $O^{16}(He^3, \alpha)O^{15}$ dominates the spectrum in its vicinity due to its much larger cross section¹⁴ than the reactions under observation. This reaction was particularly annoying at 90° because the cross section increases very rapidly with decreasing He^3 energy near 2.76 MeV.¹⁴ Therefore, even the smaller oxygen content introduced at greater target depths during the evaporation and induction heating produces a sizable tail at 90° on the low-alpha-energy side of the surface peak. The dashed continuation of this peak in Fig. 3 is a rough estimate of this effect. At 150° , the cross section decreases with decreasing bombarding energy, giving only a small low-energy tail.

The dashed peak at $V_m = 0.316$ in Fig. 2 could be made to appear by insertion of hydrogen gas into the ion source, as mentioned earlier. The group disappeared completely with pure helium in the ion bottle.

In those cases where different reaction groups overlapped, such as $N^{15}(He^3, \alpha)N^{14}$ (7.03 MeV) and $N^{14}(He^3, \alpha)N^{13}$ (7.17 MeV), a comparison of the yields of the two targets revealed the relative contributions of the two reactions. Comparison of Figs. 2 and 3 for the case cited shows clearly the operation of the $N^{15}(He^3, \alpha)N^{14}$ (7.03 MeV) reaction.

The profiles of the two reaction groups, $N^{14}(He^3, \alpha)N^{13}$

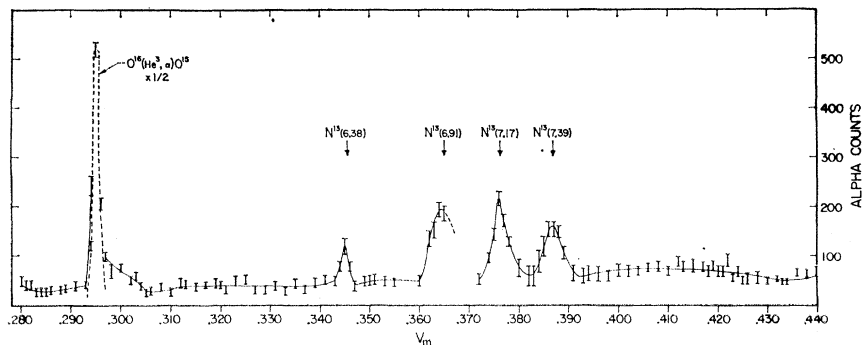
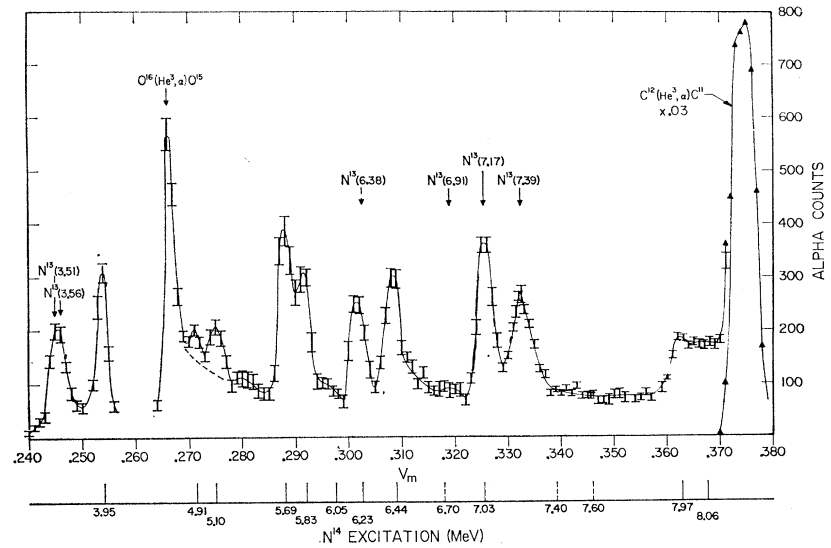


FIG. 3. The spectrum of alpha particles at $\theta_L = 150^\circ$ from bombardment of a natural nitrogen TiN target with 2.76-MeV He^3 ions. Compare Fig. 1.

¹⁴ D. A. Bromley, J. A. Kuehner, and E. Almquist, Nuclear Phys. 13, 1 (1959).

FIG. 4. The spectrum of alpha particles at $\theta_L=90^\circ$ from bombardment of 67% N^{15} target of TiN with 2.76-MeV He^3 ions.



(6.91 MeV) and $N^{14}(\text{He}^3, \alpha)N^{13}$ (7.39 MeV), have sufficient energy width to allow calculation of the widths of the final states. For N^{13} (6.91 MeV), $\Gamma=110\pm 15$ keV, and for N^{13} (7.39 MeV), $\Gamma=45\pm 10$ keV.

Table II shows the final states populated by this reaction with their measured excitation energies and the laboratory differential cross sections in microbarns per steradian at a bombarding energy of 2.763 MeV.

Of particular interest in the spectra are the expected alpha-particle groups which do not appear. Foremost among these is the reported state of astrophysical interest at 7.60-MeV excitation of N^{14} . An upper limit to the cross sections of weakly populated states near these excitation energies can be placed in the vicinity of 5 to 10 μb per sr. Such a low cross section would be an order of magnitude smaller than the cross sections to the

known states. Although such a situation is certainly possible, it would seem to be quite unlikely to occur at both angles reported, especially so in the light of the competing reaction mechanisms which allow population of the various final states. In this latter regard, it is of interest to note that the state at 6.23 MeV in N^{14} , believed to be a two-particle excitation from the p -shell ground state,⁹ is strongly populated in this reaction although it is only weakly populated by the inelastic scattering experiments. For this reason the absence of states at 6.70, 7.40, and 7.60 MeV in this experiment is a more negative result than the absence of these states in the inelastic scattering of alpha particles from N^{14} .

It was also hoped that the famous missing pair of states in N^{13} would be seen from the $N^{14}(\text{He}^3, \alpha)N^{13}$ reaction. These states would be the analogs of the states in C^{13} at 5.51- and 6.10-MeV excitation and would be expected to appear in the 5–6 MeV excitation range of N^{13} . However, no conspicuous and unexpected alpha group was observed. In particular, Fig. 3 reveals a very uneventful alpha spectrum from $V_m=0.280$ to $V_m=0.340$ except for the contaminant oxygen group and its low-energy tail. This range covers the 4.0–6.3 MeV excitation range of N^{13} .

There is a rather sizable continuum of alpha particles upon which the sharply defined groups are superposed, which is tentatively attributed to the presence of N^{14} in the target, which will allow the population of a large variety of alpha unstable states of O^{16} from the reaction $N^{14}(\text{He}^3, p)O^{16}$. The subsequent breakup would produce very broad and unresolvable alpha-particle groups throughout the energy range observed. This continuum background was consistently larger with the N^{14} target than with the N^{15} enriched target. Although alpha unstable states are also produced by $N^{15}(\text{He}^3, p)O^{17}$, these states will preferentially break up by neutron emission,

TABLE II. Final-state excitation energies and laboratory differential cross sections in microbarns per steradian for resolved alpha groups from $N^{15}(\text{He}^3, \alpha)N^{14*}$ and $N^{14}(\text{He}^3, \alpha)N^{13*}$ at a bombarding energy of 2.76 MeV.

$E_x(N^{14})$	$\frac{d\sigma}{d\Omega}(\theta_L=150^\circ)$	$\frac{d\sigma}{d\Omega}(\theta_L=90^\circ)$
3.95	64 ± 15	165 ± 20
4.91	19 ± 5	18 ± 18
		-10
5.113 ± 0.008	85 ± 15	55 ± 30
5.691 ± 0.008	340 ± 30	215 ± 30
5.832 ± 0.008	420 ± 30	180 ± 30
6.048 ± 0.012	36 ± 10	<20
6.224 ± 0.012	52 ± 15	85 ± 25
6.436 ± 0.012	160 ± 20	180 ± 20
7.032 ± 0.010	77 ± 25	135 ± 40
7.97	21 ± 10	45 ± 20
8.06	54 ± 20	45 ± 30
$E_x(N^{13})$		
6.38	40 ± 15	150 ± 30
6.91	115 ± 25	<30
7.166 ± 0.008	110 ± 25	115 ± 30
7.388 ± 0.008	70 ± 25	320 ± 60

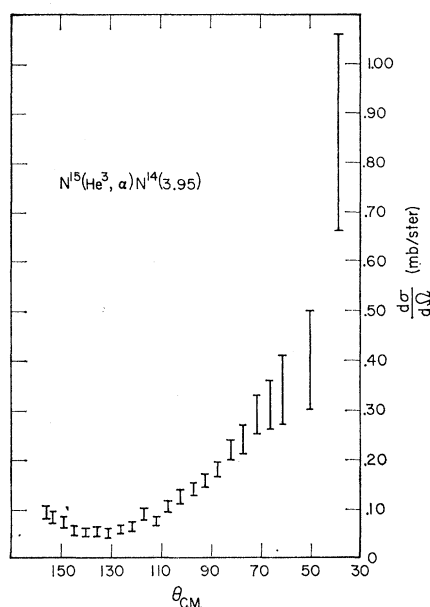


FIG. 5. The center of mass angular distribution of the alpha-particle group from $N^{15}(\text{He}^3, \alpha)N^{14}$ (3.95 MeV) at laboratory bombarding energy of 2.76 MeV.

Note added in proof. Some doubt may remain concerning the existence of an N^{14} state at 6.05 MeV excitation. The clearly resolvable group in the 150° spectrum (Fig. 2) could not be ascribed to any expected contaminants. A corresponding group is not resolvable at 90° (Fig. 4) if it is present. A subsequent spectrum taken at 120° did show a small resolvable group of the proper energy.

VI. ANGULAR DISTRIBUTIONS

It would be expected that the alpha groups from $N^{15}(\text{He}^3, \alpha)N^{14}$ should show markedly dissimilar angular distributions for groups being populated by different re-

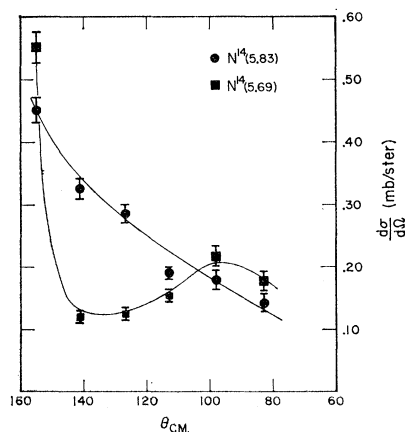


FIG. 6. The center of mass angular distribution of the alpha-particle groups from $N^{15}(\text{He}^3, \alpha)N^{14}$ (5.69 MeV) and $N^{15}(\text{He}^3, \alpha)N^{14}$ (5.83 MeV) at laboratory bombarding energy of 2.76 MeV. The curves are a visual aid only.

action mechanisms. To obtain qualitative information of this type, partial angular distributions were obtained for three alpha groups. There are very few groups that are cleanly resolved at all angles from contaminant groups so the choice was somewhat limited. The possibility of measuring angular distributions was also severely limited at forward angles due to the nature of the targets. It is quite difficult to prepare thin self-supporting nitrogen targets suitable for transmission experiments, so the angular distributions were taken in reflection geometry with the solidly backed targets described earlier. The geometric uncertainties introduced by this procedure were minimized by simultaneously performing the well-known $N^{15}(p, \alpha_0)C^{12}$ angular distributions as a normalizing standard.

The alpha group from $N^{15}(\text{He}^3, \alpha)N^{14}$ (3.95 MeV) was resolved at all angles from contaminant groups. This final state belongs predominantly to the configuration $s^4 p_{3/2}^7 p_{1/2}^3$ and can therefore be populated by the pickup of a $p_{3/2}$ neutron from the N^{15} ground state, $s^4 p_{3/2}^8 p_{1/2}^3$. The large Q value provides a large momentum transfer at all angles, so that the semiclassical active cylinder¹⁵

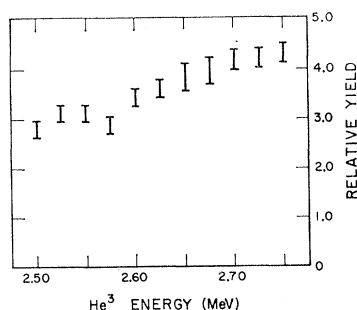


FIG. 7. Cross section for $N^{15}(\text{He}^3, \alpha)N^{14}$ (5.69 MeV) reaction at $\theta_L = 90^\circ$ as a function of bombarding energy.

intersects the nucleus even at 0° for p -wave pickup. It would therefore be reasonable to expect an angular distribution peaked in a strongly forward direction. Figure 5 shows the distribution obtained at a bombarding energy of 2.763 MeV. The small error bars at back angles represent counting statistics, whereas the increasingly large error bars at forward angles represent the uncertainty introduced by geometric effects. Although the forward angle uncertainties are great, the angular distribution certainly shows the expected general shape. It was, of course, impossible to determine whether the cross section peaked at an angle greater than 0° due to the target problem. It would be expected that the ground state and first excited state angular distributions would be similar to this one.

The alpha-particle groups to N^{14} final states at 5.69 and 5.83 MeV were also clear of contaminant groups, although they began to overlap each other badly at forward angles. Nonetheless, partial angular distributions were obtained and are shown in Fig. 6. The contrast to

¹⁵ S. T. Butler, N. Austern, and C. Pearson, Phys. Rev. 112, 1127 (1958).

the previous distribution is immediately obvious, as both of these groups show very large back-angle peaks that are characteristic of the heavy-particle stripping mechanism. Neither of these states can be populated by the neutron-pickup mechanism if they are describable as single-particle excited states from the p -shell ground state, as concluded by Warburton and Pinkston.⁹ Since the angular distribution of the 5.69-MeV level could be symmetric about 90° , a 90° excitation curve is included in Fig. 7. It shows no evidence of strong resonance structure. It seems likely that heavy-particle stripping is dominating these two reactions. It is also worth noting that the cross sections for these two reactions are considerably larger than the average.

It is surprising that the pair of states at 4.91 and 5.10 MeV, which belong to the same configurations⁹ as the 5.69- and 5.83-MeV pair, respectively, but couple to different spins, have such comparatively small cross sections for population by this reaction. Perhaps the clustering amplitudes for heavy-particle stripping are considerably larger for the angular momentum couplings associated with the higher lying pair of final states.

VII. CONCLUSIONS

On the basis of this experiment, the existence of states in N^{14} at 6.70-, 7.40-, and 7.60-MeV excitation is to be doubted. The absence of a state near 7.60 MeV means that the extrapolation of the $C^{13}(p, \gamma)N^{14}$ reaction rate to the low energy of stellar interiors made on the assumption that no resonance exists for low proton energies is correct. The minimum observed C^{12}/C^{13} abundance ratios are then consistent with the value to be expected from the CNO cycle. Alternatively, of course, one could interpret the large amounts of C^{13} observed in the cool carbon stars as evidence that the $C^{13}(p, \gamma)N^{14}$ reaction is nonresonant at low energies. Because of the conflicting evidence regarding the N^{14} energy levels, however, it is important that the $N^{14}(p, p')N^{14*}$ reaction be repeated with more modern techniques to either confirm or refute the earlier evidence for these states.

ACKNOWLEDGMENTS

The author would like to thank Professor W. A. Fowler for suggesting this experiment and Dr. D. F. Hebbard for providing the targets.

Reaction Mechanism in $Mg^{24}(p, p'\gamma)$ at Low Energies*

W. T. JOYNER

Department of Physics, Hampden-Sydney College, Hampden-Sydney, Virginia

(Received April 13, 1962)

The excitation function for the inelastic scattering of protons to the first level of Mg^{24} has been measured for bombarding energies between 2.7 and 4.2 MeV, using an electrostatic accelerator. The 1.37-MeV gamma rays resulting from inelastic scattering were measured at 0° . Six resonances occur in this energy interval, corresponding to levels in Al^{25} at excitation energies of 4.93, 5.09, 5.14, 5.75, 5.81, and 6.15 MeV. Angular distribution measurements were made of the two reaction products, both on and off resonance, and the coefficients of the Legendre polynomial expansions determined. The character of the distributions indicates the adequacy of the compound nucleus model with no evidence of direct interaction effects; the nuclear barrier height thus seems to set an approximate lower limit for the onset of direct interactions. The use of an electrostatic analyzer allowed an energy resolution of 0.05%, and calibration against the $Li(p, n)$ threshold resulted in an absolute energy uncertainty of ± 2 keV; this energy calibration allows some simplification of the level scheme in Al^{25} , particularly for excitation energies near 5 MeV.

INTRODUCTION

A NUMBER of reports have appeared recently concerning the reaction mechanism involved in the inelastic scattering of protons at low energy.¹⁻⁴ The nucleus Mg^{24} is of particular interest because of the low

binding energy for an added proton, (2.29 MeV), allowing one to reach low-lying, widely separated levels in the compound nucleus when low bombarding energies are used. For energies below 3 MeV, Litherland *et al.*⁵ have found their results to be well fitted by a collective model which ascribes a prolate distortion to the Mg^{24} ground state. The excitation is then described as a collective excitation of the nucleus, causing it to rotate or vibrate about its spheroidal ground-state shape. For bombarding energies near 7 MeV, Seward interprets his results as indicating a direct interaction of the type

* Supported by the U. S. Atomic Energy Commission at Duke University.

¹ Frederick D. Seward, Phys. Rev. **114**, 514 (1959).

² H. A. Lackner, G. F. Dell, and J. Hausman, Phys. Rev. **114**, 560 (1959).

³ H. J. Hausman, G. F. Dell, and H. F. Bowsher, Phys. Rev. **118**, 1237 (1960).

⁴ H. F. Bowsher, G. F. Dell, and H. J. Hausman, Phys. Rev. **121**, 1504 (1961).

⁵ A. E. Litherland, E. B. Paul, G. A. Bartholomew, and H. E. Gove, Phys. Rev. **102**, 208 (1956).